arXiv:astro-ph/9906343v1 22 Jun 1999

The heating of the ICM by powerful radio sources

C. R. Kaiser[1] **and P. Alexander**[2]

[1] Max–Planck–Institut für Astrophysik, Karl-Schwarzschild-Str.1, 85740 Garching, Germany
[2] Cavendish Laboratory, Madingley Road, Cambridge, CB3 0HE, UK

Abstract. We present a model for the compression and heating of the ICM by powerful radio galaxies and quasars. Based on a self-similar model of the dynamical evolution of FRII-type objects we numerically integrate the hydrodynamic equations governing the flow of the shocked ICM in between the bow shock and the radio lobes of these sources. The resulting gas properties are presented and discussed. The X-ray emission of the shocked gas is calculated and is found to be in agreement with observations. The enhancement of the X-ray emission of cluster gas due to the presence of powerful radio galaxies may play an important role in the direct detection of cluster gas at high redshifts.

1. Introduction

Since jets were identified as the means by which AGN transport their energy to the large scale structure of radio galaxies and radio loud quasars observed at radio wavelengths (Rees 1971, Scheuer 1974), much effort has been devoted to the question how the environments of the hosts of extragalactic radio sources influence the evolution of these objects. On the other hand, the influence of powerful radio sources on the properties and the evolution of their environments is still largely unknown. This is partly caused by the difficulty involved in observing the interaction of the large scale structure of radio sources with its surroundings.

In the case of the lower luminosity version of radio galaxies (type FRI, Fanaroff & Riley 1974) high resolution radio maps show a very complex and turbulent jet flow. This turbulence is caused by the passage of the jet through the ICM. In the case of the more powerful version (FRII) the interaction with the ICM is not so directly visible. In these objects the jets are much more collimated and end at distinct points; the radio hot spots. The lobe-like radio structure of FRII-type sources surrounding the jets is thought to expand supersonically with respect to the ICM. However, the resulting bow shock is inferred theoretically but has been detected indirectly in only one source (Carilli, Perley & Dreher 1988).

Despite this lack of directly observable signatures of the influence of radio sources on their environments, the resulting effects on the properties and the evolution of the ICM should be quite significant. The confinement of the large scale structure of radio sources of type FRII implies that a considerable fraction of the energy transported by the jets is transfered to the ICM. The shocks around the radio structures of FRII-type objects are presumably very effective at converting the expansion energy of the radio lobes into thermal energy of the ICM. Furthermore, the jets in FRIIs are found to be more powerful than those in FRI-type sources (e.g. Rawlings & Saunders 1991). This means that the 'stronger flavour' FRII radio sources may also influence the ICM more strongly.

At low redshift FRIIs are predominantly found in poor groups and rarely in clusters. However, there is some evidence that at high redshift these powerful sources are located in richer environments (e.g. Hill & Lilly 1991). This may imply that at earlier cosmological epochs FRII-type radio sources were more common in proto-cluster environments possibly influencing their evolution significantly.

In this paper we outline a model describing the interaction of FRII-type radio sources with their environments and the resulting enhancement of the X-ray emission of this material. This represents a first step towards unraveling the complex relation between the evolution of powerful active galaxies in clusters and that of their surroundings.

2. Analytical model of the evolution of FRII radio sources

It is obviously not possible to observe one source at various stages of its life thereby 'watching' the evolution of a given radio source. However, complete samples of radio galaxies and quasars provide us with a view of many sources of very different ages. If the evolution of these sources is not completely different from one another than we can hope to reconstruct some of the characteristics of this evolution. Leahy & Williams (1984) and Leahy, Muxlow & Stephens (1989) find a correlation between the radio luminosity of FRII radio galaxies of linear sizes up to 500 kpc with the aspect ratio of their radio lobes, i.e. the ratio of the lobe

widths to their lengths, R, but find no correlation of R with the linear sizes of the radio lobes. Subrahmanyan, Saripalli & Hunstead (1996) find values of R for sources exceeding 900 kpc in linear size which are very similar to the ones found for the smaller sources. This strongly suggests that the large scale structure of radio galaxies and radio loud quasars with FRII morphology grows in a self-similar fashion. Any theoretical model of the development of these structures must therefore comply to this observational constraint.

Scheuer (1974) and Begelman & Cioffi (1989) argued that the region of the radio lobes or cocoon should be overpressured with respect to the surrounding gas and will therefore drive a strong shock, the bow shock, into this material. Falle (1991) then showed that the expansion of this bow shock should be self-similar once the mass of the ICM swept up by this shock and pushed aside by the cocoon exceeds the mass of the material within the cocoon. This requirement is fulfilled for virtually any radio galaxy of a linear size exceeding a few kpc. In Kaiser & Alexander (1997) we developed a model which predicts the self-similar growth of FRII-type radio galaxies. The following is a brief summary of this model and its assumptions.

We assume that the two jets emerge symmetrically to both sides from the AGN in the centre of the host galaxy. The jets end in strong shocks. These shocks and their immediate surroundings form the observed radio hot spots. The jet material then inflates the cocoon which shields the jets from the denser material of the ICM. Because of the very high sound speeds within this post-shock material the pressure in the cocoon will equalize rapidly and so the pressure within the cocoon is uniform throughout with the exception of the hot spot region. The magnetic field in the cocoon is assumed to be tangled on scales smaller than any of the dynamically relevant scales. It therefore contributes to the overall pressure within the cocoon but does not exert any non-isotropic stresses. This implies that the jets are confined solely by the pressure within the cocoon. The source is embedded in the ICM and we model the gas density distribution within this material with a power law. This is a reasonable approximation at large radii to the more realistic King (1972) profile which provides good fits to the observed X-ray brightness profiles in the vicinity of radio galaxies and that of clusters. The cocoon expands into this material at a velocity exceeding the local sound speed. The whole radio source is therefore surrounded by a bow shock.

Using these simple assumptions we find that not only the growth of the bow shock but also that of the cocoon, i.e. the radio lobes, should be self-similar. Note that this is a result of the model and not an assumption. Furthermore, to arrive at this result we have made no assumptions about the shape of the bow shock or the cocoon. With this model we calculate that about half of the energy transported by a 'typical' jet of a radio source of type FRII is eventually converted to kinetic and thermal energy of the shocked ICM located between the bow shock and the boundary of the cocoon. The jets of a conventional radio galaxy have an energy transport rate of roughly 10^{46} ergs s^{-1}. This implies that such an object deposits about 10^{61} ergs of energy in the ICM during its lifetime of 10^8 years. This enormous amount of energy will certainly influence the subsequent evolution of any gaseous structure the radio galaxy is embedded in.

3. Shock heating of the ICM

Because we do not make any assumptions about the shape of the bow shock and the cocoon in the model described in the previous Section, it is impossible to determine from this model alone how and in which form the energy transfered from the jet to the shocked ICM is distributed. The properties of the gas in the layer in between the bow shock and the boundary of the cocoon are essentially described by the usual hydrodynamical equations; the equations of conservation of mass, momentum and energy. The problem resembles that of the gas flow behind the shock front of a strong explosion presented by Sedov and Taylor (e.g. Sedov 1959). Dyson, Falle & Perry (1980) present an extension to the explosion case in the form of a spherically symmetric wind with constant energy input driving the shock front. In both cases the solutions are self-similar. This and the results of our own model described in the previous Section encouraged us to construct a model for the layer of shocked gas surrounding the cocoons of FRII-type radio sources. The main difference to the previous work is the elongated geometry of the radio source and the therefore more complex structure of the hydrodynamical equations. The method and results presented in the following are described in more detail in Kaiser & Alexander (1999).

In their simplest form the conservation equations present a problem with four independent variables; three spatial and one time variables. To reduce the complexity we assume an adiabatic equation of state for the shocked gas and axisymmetry about the jet axis. The self-similar expansion of the cocoon and the bow shock then allows us to recast the equations in a co-moving coordinate system which expands with the bow shock and the boundary of the cocoon. In this system these two surfaces are at rest. This then reduces the number of independent variables to two spatial coordinates. Our dynamical model predicts the growth of the radio source to be self-similar independent of the exact geometrical shape of the bow shock and that of the cocoon. We are therefore free to choose a shape for either of these surfaces to fit observations. Once we have chosen a specific shape for one of these surfaces and the initial conditions along this starting surface, it is possible to numerically integrate the hydrodynamical equations in the direction of the other surface until it is reached by the solution. Although it seems natural to choose the boundary of the cocoon to start the integration from, since the

cocoon is driving the bow shock, it is more appropriate to start from the bow shock. This is because in the co-moving coordinate system the gas is apparently streaming through the bow shock into the shocked region towards the cocoon boundary. Also, if we assume the bow shock to be strong than the initial conditions of the gas just behind the bow shock are well determined. For the shape of the bow shock and therefore for that of the co-moving coordinate system we choose a prolate spheroid. The resulting shape of the cocoon boundary found from the numerical integration is very similar and therefore agrees well with observations of radio lobes. For details of the calculation and the numerical method we refer the reader to Kaiser & Alexander (1999).

4. Properties of the shocked ICM

Figure 1 shows the velocity field of the gas within the shocked layer. The gas is flowing along the boundary of the cocoon. The flow lines are bent parallel to this surface. The two stagnation points in front of the end of the jet and close to the x-axis away from the bow shock are caused by the symmetrical boundary conditions which do not allow any gas flow across the jet axis or through the surface defined by the rotation of the x-axis about the jet axis into the other half of the cocoon. The cocoon in Figure 1 is relatively broad. This is for illustrative purposes only. The flow patterns in 'slimmer' cocoons are very similar.

The distribution of the gas density within the shocked layer is shown in Figure 2 for three different density profiles of the unshocked ICM in front of the bow shock. The case of a uniform density of the ICM is qualitatively similar to the findings of Sedov (1959) and Dyson et al. (1980). The density decreases away from the bow shock towards the cocoon boundary. This is the signature of the gas that is re-expanding after being compressed by the bow shock. This general trend is much weaker in the case of $\beta = 1$ and is reversed for $\beta = 2$. In the latter case the expansion of the gas behind the bow shock is so slow that the original density distribution, i.e. decreasing density with increasing distance from the source centre, is preserved. This gives the impression of a further compression of the gas on its way from the bow shock to the cocoon boundary. It is interesting to note that this reversal of the density profile in the shocked gas is not a result of the elongated geometry of the bow shock but is also present in the spherical case (see Kaiser & Alexander 1999).

The pressure distribution within the shocked gas is presented in Figure 3. Away from the region immideatly in front of the jet end the pressure is decreasing away from the bow shock towards the cocoon for $\beta = 0$ and $\beta = 1$. This is the behaviour found by Dyson et al. (1980) in the spherical case. However, in front of the hot spot where the jet ends the pressure is increasing towards the cocoon for all three cases. We find the same pattern all along the bow shock for $\beta = 2$. The pressure at the cocoon boundary also varies along this surface. In the case of a uniform density of the unshocked ICM we find a monotonic decrease of the pressure from the hot spot region towards the x-axis. For the other cases studied here the pressure also decreases away from the hot spot but then rises again towards the x-axis. In the case of $\beta = 2$ the pressure at the cocoon boundary on the x-axis is almost as high as in front of the hot spot. This also causes the slight bend in the cocoon surface towards the jet axis in this case. The pressure at the cocoon boundary must be matched by the material inside the cocoon. The strong variation of the pressure along this surface in the case $\beta = 2$ therefore clearly violates our assumption of a uniform pressure within the cocoon. This inconsistency may imply that the cocoons of FRII sources embedded in environments with steep density gradients do not grow self-similarly or that the shape of the bow shocks in front of them is not well approximated by the prolate spheroid we have assumed here. In the second case significant off-axis flow of the radio plasma within the cocoon may occur. Note also that we have assumed an adiabatic equation of state for the shocked gas. In the high pressure - high density region close to the x-axis of sources embedded in environments with steep density gradients this approximation may not be appropriate and radiative cooling could be very effective. This would decrease the pressure in these regions and may lead to a self-consistent model also for steep external density gradients.

We have assumed that the density distribution of the unshocked ICM follows a power law. This is a good approximation to the more appropriate King (1972) profile at large radii. The King profile corresponds roughly to the equilibrium distribution of an isothermal sphere of gas. We therefore expect the temperature of the shocked gas not too vary strongly with position in the flow since the initial conditions behind the bow shock are not a very strong function of position either. Our calculations show that there are indeed no large temperature fluctuation within the layer of shocked gas. The only exception is the region in front of the hot spot where the temperature is somewhat higher than in the rest of the gas.

Since the density and the temperature of the shocked gas is known from the model, it is straightforward to calculate the X-ray surface brightness of the shocked gas layer due to thermal bremsstrahlung. For this we used the emission of the gas in the range from 0.1 to 2 keV, appropriate for the High Resolution Imager (HRI) on board ROSAT. We rotated the source about the jet axis and then calculated the surface brightness by integrating along line of sights perpendicular to the plane of the map shown here. This of course assumes that the source lies in the plane of the sky. In Figure 4 we show the results of this calculation for the three cases discussed here.

For a steep external density gradient the X-ray emission is very concentrated just behind the bow shock close to the x-axis. This can be explained with the high gas density in this region. In general the X-ray surface bright-

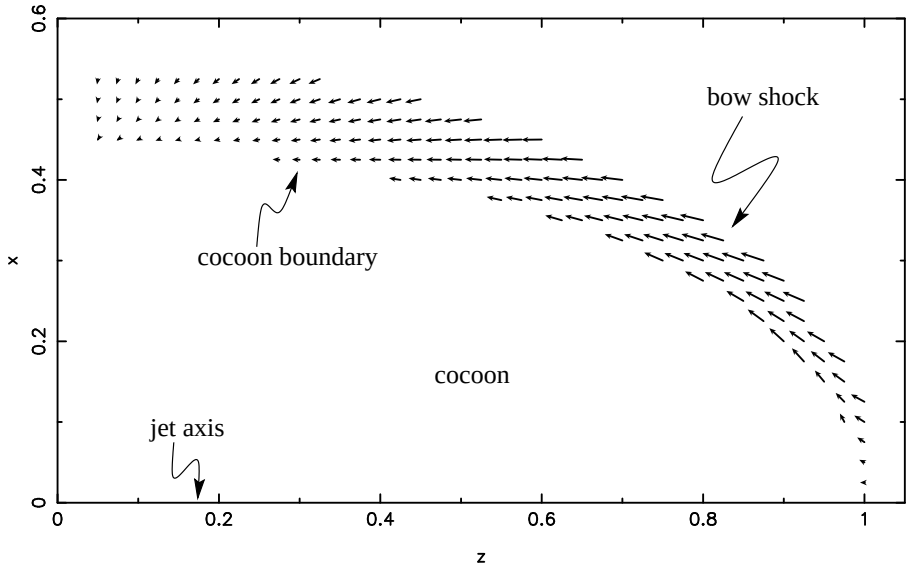

Fig. 1. The velocity field of the gas in the shocked layer in between bow shock and cocoon. In this and the other figures we only show one quarter of the radio source. Because of the assumed rotational symmetry about the jet axis all velocity vectors are not projected and lie fully in the plane of the plot. The centre of the host galaxy is located at the origin of the plot while the jet ends roughly at x=0 and z=1. The velocities are shown in the rest frame of the cocoon boundary and the bow shock. The axes are in units of the cocoon length.

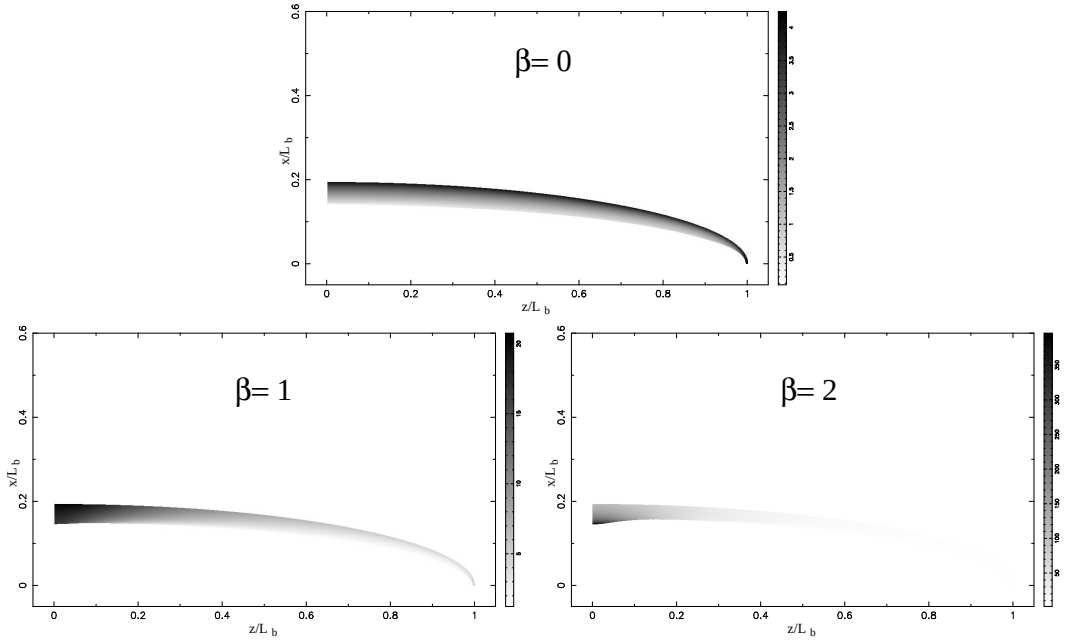

Fig. 2. The density distribution of the shocked gas in between the bow shock and the cocoon boundary. β is the exponent of the power law describing the density profile of the unshocked ICM in front of the bow shock.

ness is predicted by our model to be a good tracer of gas density. However, this of course is mainly due to the assumption of an isothermal sphere for the unshocked gas. If temperature fluctuations are present in the unshocked ICM, they will disturb the rather smooth result presented here.

The only FRII-type radio galaxy which has been observed with enough spatial resolution and sensitivity to detect this emission from the shocked ICM to date is Cygnus A. The HRI map presented by Carilli, Perley & Harris (1994) shows an enhancement of the X-ray emission in the correct place; along the radio lobes close to the core of the host galaxy. A more quantitative analysis of the

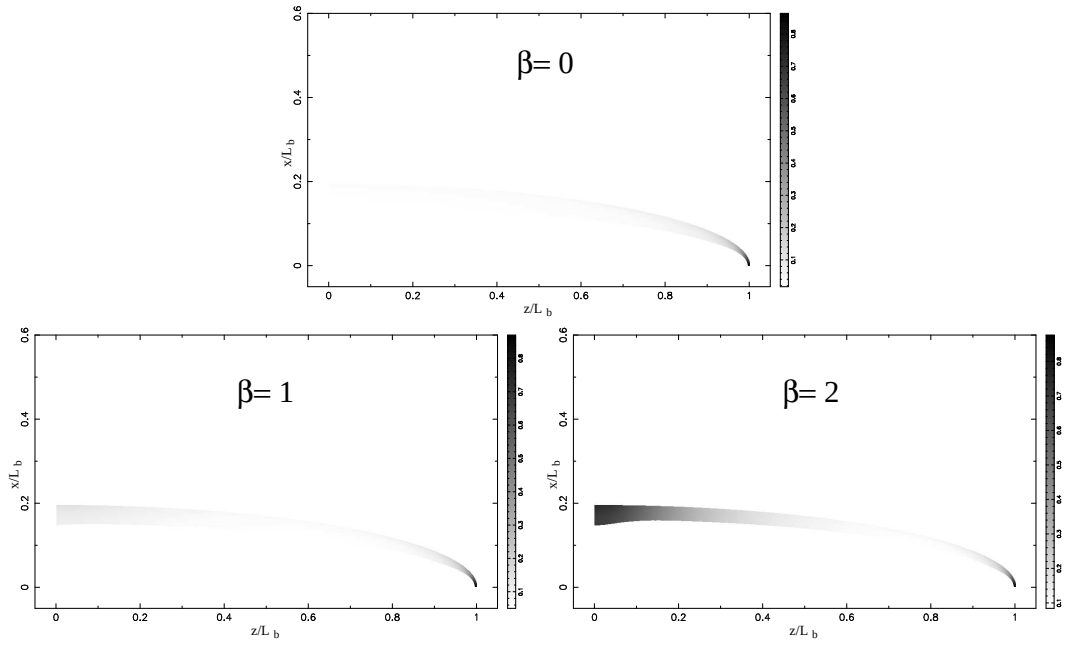

Fig. 3. The pressure distribution of the shocked gas in between bow shock and cocoon boundary.

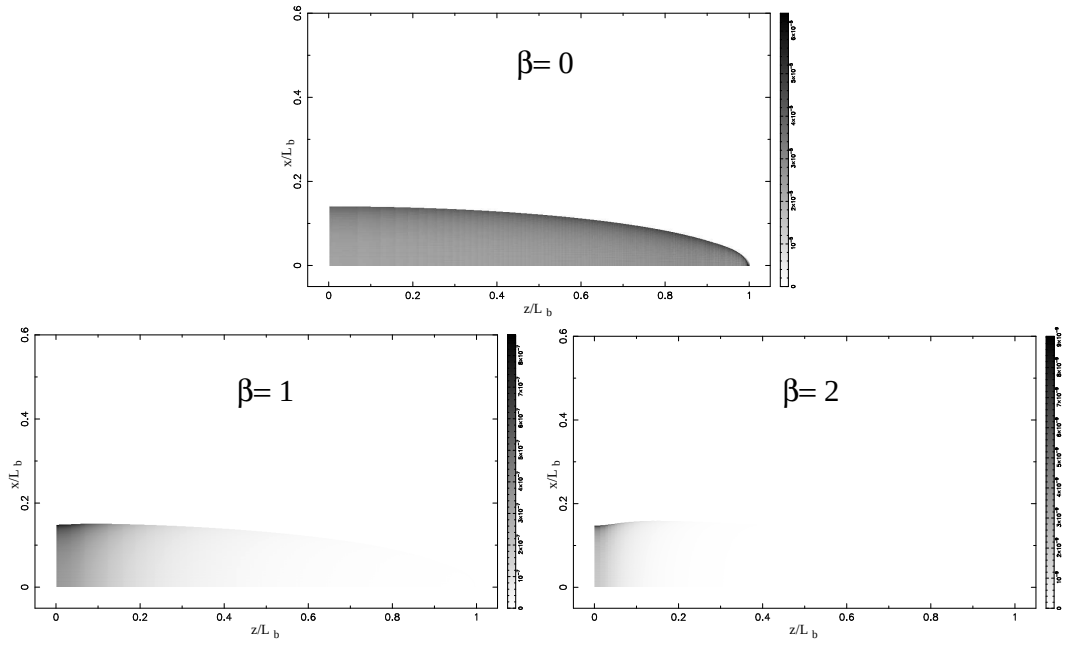

Fig. 4. The X-ray surface brightness in the 0.1 to 2 keV band.

X-ray map in this case is difficult because the presence of the radio source precludes an accurate determination of the properties of the unshocked IGM. However, using the model outlined above we find some evidence that the gas causing the mentioned X-ray emission peaks may have been denser than expected at this position from a pure King profile before it passed through the bow shock. Additional radiative cooling in these regions as outlined above may also contribute to the higher density here.

Another intriguing example for a possible detection of enhanced X-ray emission of shocked gas due to the effects of jets is the HRI map of the possible cluster around the powerful radio galaxy 3C 356 by Crawford & Fabian (1996). The distance of this object (z=1.079) is far too great to allow an observation as well resolved as the one of Cygnus A. However, the possible extension of the X-ray detection is well aligned with the axis of the radio source as we would expect from our model. The heating of the ICM by powerful radio sources together with the

scattering of nuclear emission from the AGN (Setti, these proceedings) may therefore play an important role in the direct detection of high redshift clusters because both processes enhance the X-ray emission of the cluster gas.

5. Summary

We have presented an analytical model for the dynamical evolution of powerful extragalactic radio sources of type FRII. This model predicts self-similar growth of the bow shock and radio lobes/cocoon of the sources independent of the exact geometrical shape of these surfaces. Based on this model we performed a numerical integration of the hydrodynamical equations governing the gas flow of the shocked ICM between the bow shock and the boundary of the cocoon of FRII sources. We find that the X-ray surface brightness of the shocked gas is boosted significantly by the presence of the shock. In the case of an initially isothermal density distribution of the ICM the enhanced X-ray surface brightness distribution is a good tracer of gas density within the shocked layer of gas. The model is in agreement with the high resolution X-ray observations of Cygnus A.

The presence of a powerful radio source in a cluster clearly boosts the X-ray emission of the ICM. This may help us in detecting this material at high redshifts. The influence of radio sources on the evolution of the ICM still remains to be investigated in detail. The study presented here is a first step towards this goal.

References

Begelman M. C., Cioffi D. F., 1989, ApJ, 345, L21
Carilli C. L., Perley R. A., Dreher J. H., 1988, ApJ, 334, L73
Carilli C. L., Perley R. A., Harris D. E., 1994, MNRAS, 270, 173
Crawford C. S., Fabian A. C., 1996, MNRAS, 281, L5
Dyson J. E., Falle S. A. E. G., Perry J. J., 1980, MNRAS, 191, 785
Falle S. A. E. G., 1991, MNRAS, 250, 581
Fanaroff B. L., Riley J. M., 1974, MNRAS, 167, 31
Hill G. J., Lilly S. J., 1991, ApJ, 367, 1
Kaiser C. R., Alexander P., 1997, MNRAS, 286, 215
Kaiser C. R., Alexander P., 1999, MNRAS, 305, 707
King I. R., 1972, ApJ, 174, L123
Leahy J. P., Williams A. G., 1984, MNRAS, 210, 929
Leahy J. P., Muxlow T. W. B., Stephens P. W., 1989, MNRAS, 239, 401
Rawlings S., Saunders R., 1991, Nat., 349, 138
Rees M. J., 1971, Nat., 229, 312
Scheuer P. A. G., 1974, MNRAS, 166, 513
Sedov L. I., 1959, Similarity and dimensional methods in mechanics. Academic Press, London
Subrahmanyan R., Saripalli L., Hunstead R. W., 1996, MNRAS, 279, 257